Detection of the Meissner effect with a diamond magnetometer

Louis-S Bouchard[1,3]**, Victor M Acosta**[2]**, Erik Bauch**[2]
and Dmitry Budker[2]

[1] Department of Chemistry and Biochemistry, California NanoSystems Institute, Biomedical Engineering IDP, Jonsson Comprehensive Cancer Center, University of California, Los Angeles, CA 90095, USA
[2] Department of Physics, University of California, Berkeley, CA 94720-7300, USA
E-mail: bouchard@chem.ucla.edu

Abstract. We examine the possibility of probing superconductivity effects in metal nanoclusters via diamond magnetometry. Metal nanoclusters have been proposed as constitutive elements of high-T_c superconducting nanostructured materials. Magnetometry based on the detection of spin-selective fluorescence of nitrogen-vacancy (NV) centers in diamond is capable of nanoscale spatial resolution and can be used as a tool for investigating the properties of single or multiple clusters interacting among each other or with a surface. We have carried out sensitivity estimates and experiments to understand how these magnetometers could be used in such a situation. We detected the flux exclusion effect in a superconductor by monitoring the magnetic resonance spectrum of a large ensemble of NV centers in diamond. Our results show that phase transitions can be ascertained in a bulk superconductor with this technique. We also discovered temperature-dependent behavior of the zero-field splitting parameter D and conclude that the general implementation of such measurements may require compensation schemes.

Superconductivity occurs in a wide variety of materials when the temperature drops below a critical temperature T_c and is accompanied by diamagnetism and a drop in resistance to electric current. The superconducting transitions observed to date are all below 135 K, under

---

[3] Author to whom any correspondence should be addressed.

normal atmospheric pressure, and they are mostly associated with bulk systems. In recent years, the search for room-temperature superconductivity has been approached from several different angles [1], including searching for systems with negative dielectric functions [2], synthesizing crystals with specific phonon spectra [3], creating materials with a pore structure [4] and studying the superconducting state at interfaces in epitaxial heterostructures [5].

Metal nanoclusters, which can exhibit superconductivity effects [6]–[8], also form a novel family and could potentially develop into room-temperature superconductors. Size-selected metal nanoclusters, in the case of certain metals, are known to exhibit an electronic shell structure [6]–[8]. Kresin and Ovchinnikov recently proposed that a superconducting transition can occur for some metal nanoclusters with 10^2–10^3 valence electrons [9, 10]. The transitions are expected to occur near electronic shell closings. Under special circumstances, the shell structure is expected to strengthen pairing correlations and leads to elevated values for the critical temperature for a transition to the superconducting state. The superconducting state of small nanoclusters is directly related to the phenomenon of pair correlation. Recently, Cao *et al* [11] have presented experimental measurements of a jump in the heat capacity of Al_{45}^- and Al_{47}^- clusters, which is strong evidence of a superconducting transition in isolated clusters. The transition temperature was $T_c \approx 200\,\mathrm{K}$. A number of interesting predictions for other clusters have been made in [9, 10].

The clusters' exceedingly small sizes (1 nm or less) make them difficult to study in the laboratory, as they are inaccessible to a large number of common spectroscopies and methods for detecting superconductivity. It is important to have additional means to probe such clusters on an individual level and in populations, so that cluster–cluster or cluster–surface interactions can be studied. Recent developments in solid-state magnetometers, such as anisotropic magnetoresistive sensors [12, 13] or those based on diamonds with nitrogen-vacancy (NV) color centers [14]–[16], have opened up new possibilities for sensitive magnetic measurements of material properties over a broad range of temperatures and with high spatial resolution. 'NV-diamond' magnetometers have been developed that can perform measurements at the nanoscale, potentially with single-spin detection [14, 16].

In this paper, we look at the feasibility of performing magnetic measurements near the surface of a superconductor to detect the phase transition through the Meissner effect or flux exclusion. There are three common approaches to finding the critical temperature in superconductors. These consist of measurements of magnetic susceptibility, electrical resistivity and heat capacity. Resistivity measurements at the nanoscale are challenging. Very often, more than one type of experimental measurement is needed in order to convincingly prove the existence and probe the nature of the superconducting state. For heat capacity measurements in individual isolated clusters, we refer to the recent work of Jarrold and co-workers [17, 18]. Susceptibility measurements report changes in the magnetic moment below T_c by way of a susceptometer instrument. The measurement directly probes the Meissner effect in which a transition to diamagnetism occurs.

Diamagnetism in metal clusters is different from that in bulk metals. Clusters containing a magic number of electrons (i.e. filled shell) are diamagnetic regardless of the pairing correlation because of the spherical symmetry of the electronic shell structure [9]. This is an important deviation from bulk superconductors, which suggests the lack of a detectable Meissner effect.

For clusters with incomplete shells, however, there is orbital paramagnetism at high temperatures [9] and the transition to the superconducting state at $T = T_c$ should be

accompanied by the paramagnetic–diamagnetic transition in the cluster moment. This suggests that there may be a detectable Meissner effect. On the other hand, the London penetration depth for bulk superconductors (typical values are between 50 and 500 nm) is generally much larger than the cluster sizes recently proposed for room-temperature superconductivity [10].

It may be unclear at first glance whether a Meissner effect could be observed via magnetometry experiments in single clusters, and what is the cluster size below which it would become unobservable. The concept of a penetration depth is associated with a Landau theory for bulk superconductors. Here, we are dealing with a cluster that is characterized by an electronic shell structure rather than bulk properties. For such clusters, the transition to the superconducting state is fundamentally different [10].

In cluster crystals or suspensions of clusters in an embedding medium, the situation is likely to be different from that of single clusters because of proximity effects. In [19], for example, the Meissner effect was observed for Pb nanoparticles embedded in an organic matrix. Alternative methods of detection that could be implemented by diamond magnetometry include measurements of the Knight shift or spin relaxation times, both of which are known to be indicators of the superconducting phase transition. For example, T_1 exhibits the Slichter–Hebel peak below T_c [20]. T_1 could also be used, in favorable cases, to report on the phonon spectrum (see e.g. [21]) and this would be useful for probing electron–phonon coupling mechanisms.

The development of bulk room-temperature superconductors out of atomic or molecular clusters may require a three-dimensional (3D) assembly of clusters into a lattice structure. Such 3D assembly into cluster crystals has been demonstrated in [22]. The study of individual clusters may be best performed by immobilizing individual clusters on a surface. Recently, 'softlanding' of Ag_{561} clusters on a C_{60} monolayer has been demonstrated [23]. Another group has succeeded in immobilizing clusters on a surface [24] by accurate placement and dimensional control in the assembly of clusters. This method would enable precise control of the number and position of clusters assembled on a surface, leading to a more systematic way to perform experiments that probe cluster–cluster interactions.

Magnetic moments of atomic clusters are usually measured in beam experiments using Stern–Gerlach deflection [25]. An interesting variant would use surface magnetic measurements to probe the cluster while it interacts with the surface or in the presence of an embedding material. Probing single clusters rather than populations would enable us to study heterogeneity in the properties among an ensemble of clusters rather than measuring ensemble-averaged properties. In addition to superconductivity and magnetism, one could also probe insulator-to-metal transitions as a function of cluster size and temperature. As atoms are added to the cluster, the number of delocalized electrons increases and the cluster's initially paramagnetic state fluctuates and eventually becomes diamagnetic.

The magnetic properties (magnetization, M) of magnetic materials are often measured with a susceptometer under an applied field (B). The M–B curve is typically probed using a SQUID (superconducting quantum interference device) gradiometer oscillated sinusoidally near the sample and cycling the applied field. For clusters, a similar kind of experiment may be possible in which a bias field generates a strong enough magnetic polarization M to observe the diamagnetism/paramagnetism of the cluster at the sensor's location. Let us consider the example of an Na_{92} cluster ($N = 92$) placed in a magnetic field, $B = 1$ T. Assuming spherical clusters, the magnetic moment of a diamagnetic cluster is given by the formula [26]

$$\mu_{\mathrm{dia}} = -\frac{e^2 B}{6m} N \langle R^2 \rangle, \tag{1}$$

where $R = a_0 r_s N^{1/3} \approx 9.32 \times 10^{-10}$ m for Na$_{92}$, r_s is the Wigner–Seitz radius, a_0 is the Bohr radius and m and e are the mass and charge of the electron, respectively. This leads to $\mu_{\mathrm{dia}} = -3.8 \times 10^{-25}$ A m^2. If the sensor is placed at a distance of 10 nm from the cluster, the induced field to be measured for the diamagnetic state is

$$B_{\mathrm{dia}} \approx \frac{\mu_0}{4\pi} \frac{\mu_{\mathrm{dia}}}{r^3} \approx -3.8 \times 10^{-8} \, \mathrm{T}, \tag{2}$$

or $B_{\mathrm{dia}} \approx 3.8 \times 10^{-5}$ T at 1 nm distance.

In the paramagnetic state, we can apply the formula of Pauli paramagnetism for a free electron gas, which gives [26]

$$M = \frac{n\mu_{\mathrm{B}}^2}{E_{\mathrm{F}}} B, \tag{3}$$

where n in this formula is the number of atoms per unit volume, namely $n = 0.97 \, \mathrm{mol}/22.989 \, \mathrm{cm}^3$ for sodium metal, μ_{B} is the Bohr magneton and the Fermi energy for Na is $E_{\mathrm{F}} = k_{\mathrm{B}} T_{\mathrm{F}} = 3.24$ eV.

This gives a magnetization of $M = \chi_{\mathrm{para}} B \approx 0.7 \times 10^{-5}$ T in a 1 T applied field. The corresponding dipole moment is

$$\mu_{\mathrm{para}} = M \cdot V \approx 1.94 \times 10^{-26} \, \mathrm{A} \, \mathrm{m}^2, \tag{4}$$

where $V = 3.1 \times 10^{-27}$ m^3 is the volume of the Na$_{92}$ cluster. The corresponding dipole field is

$$B \approx \frac{\mu_0}{4\pi} \frac{\mu_{\mathrm{para}}}{r^3} \approx 2 \times 10^{-9} \, \mathrm{T} \tag{5}$$

at 10 nm separation distance, or $B \approx 2 \times 10^{-6}$ T at 1 nm distance. To measure a field of magnitude 10^{-9} T with a sensor whose noise floor is $4 \, \mathrm{nT}/\sqrt{\mathrm{Hz}}$ requires about 8 s of averaging[4]. We note that although the paramagnetism is less than the diamagnetism, the phase transition is predicted to be accompanied by a shift from paramagnetic to diamagnetic states upon crossing T_{c}. This is only true of clusters. Indeed, diamagnetism in metal clusters is different from that in bulk metals. A Meissner effect may be observable in clusters with incomplete shells, due to paramagnetism at high temperatures [9], and the transition to the superconducting state should be accompanied by the paramagnetic–diamagnetic transition in the cluster moment.

A number of considerations arise for NV-based sensors when a large external field is applied, for example: (i) the high fields required, (ii) the field drift, (iii) alignment of the NV centers and (iv) the background magnetism of the substrate. (i) While microwave sources are available for use in high fields, high fields could lead to lower optical polarization. It is encouraging to see that Neumann *et al* [27] successfully interrogated NV centers in diamond under a bias field of 0.65 T. (ii) Long-term drift of a magnet is not a problem because optically detected magnetic resonance (ODMR) measurements can be carried out over shorter timescales. Problems may arise with unstable magnets if they exhibit high-frequency drifts. Superconducting and permanent magnets are generally free of such high-frequency drifts. (iii) Previous work has shown that misalignment of the external field with respect to the NV crystal axis can lead to lower NV spin coherence times [28] and reduced optically induced spin polarization [29]. However, these effects are minimal for misalignments of the order of 1°, and

---

[4] We note that this level of sensitivity was measured for single NV centers in bulk diamond far away from the surface. It is likely that NV centers near the surface of diamond have less favorable coherence times. This is a situation where ac magnetometry and dynamic decoupling sequences may prove extremely helpful [27, 44, 45].

therefore the alignment of the magnetic field with the NV axis, although a legitimate concern in high fields, is not an insurmountable obstacle. (iv) The background magnetism of the substrate can be mitigated by translating the measuring tip near the cluster and performing subtraction of the signal from neighboring points (see figure 1(B)) [14]. This technique has been successfully implemented in scanning probe micro-SQUID susceptometers [30].

If the Zeeman effect exceeds the zero-field splitting (ZFS), the fine structure becomes a small perturbation, so all NV orientations will have similar ground-state structure (with e.g. $\sim$GHz corrections on top of the ~ 10 GHz ESR frequencies). The most serious issues may have to do with reduced optical polarization for fields $\gtrsim 1$ T that are misaligned with the NV axis. In this regime, spin–orbit and orbit–vibration coupling in the excited levels must be considered.

A potential additional contribution to the magnetism from a cluster is nuclear magnetism, which could produce a net magnetic field comparable to that from electronic paramagnetism. In some situations, stable nonmagnetic nuclear isotopes (such as ^{96}Rh) can be employed. If nonmagnetic isotopes are not available, measures should be undertaken to mitigate the effects of nuclear polarization and nuclear-spin noise. One possibility is to randomize or rotate the nuclear moments with an oscillating (ac) field if the T_1 is long compared to the duration of the ODMR readout. For short nuclear-spin T_1, repeated measurements will lead to an averaging of the spin noise.

A comment is in order pertaining to the absorption of radiation by the superconducting cluster. If the NV-diamond sensor is placed in close proximity to the cluster, the absorption of photons from the incident laser beam may present a problem. In clusters, the superconducting energy gap is substantially larger than in the bulk (e.g. 80 meV for a typical cluster), but not large compared to optical wavelengths. The absorption of optical radiation will lead to quasiparticle excitation. However, the relaxation time of the order parameter is in the picosecond range [31], so the return to the superconducting state will be a near certainty relative to the timescale of the ODMR experiment. It may also be possible to slightly reduce the photon–cluster interaction by attenuating the radiation using a polymer coating. Coatings as thin as 4 nm have been realized using the method of plasma polymerization [32].

As to a possible quenching of the fluorescence from the presence of the metal cluster, we anticipate this to be a remote possibility. Only a small number of metals are known to be good fluorescence quenchers. For example, gold is a good fluorescence quencher due to the broad plasmon resonance [33]. However, interest in gold as a candidate for high-temperature superconductivity is nearly nonexistent due to a poor pairing mechanism mediated by the electron–phonon interaction.

A number of possible surface effects may arise. For example, it is at present unknown whether NV centers with long coherence times can be obtained near the surface of diamond. We also do not know whether the interaction with the sample surface will affect these coherence times.

We also note that in a cryogenic environment the photon collection efficiency is often considerably less than ideal. Some strategies have been introduced to fight this problem [34, 35]. It may be less of an issue with the clusters of interest that have T_c's well above (e.g. 200 K) the cryogenic temperatures where photon collection efficiency is an issue.

A possible experimental setup for interrogating atomic clusters and cluster crystals is shown in figure 1(A). A nanoscale diamond tip is positioned near the surface of the cluster crystal or immobilized clusters and the tip is scanned along the surface to provide spatially resolved information. The magnetic field gradient can be measured by scanning the tip across
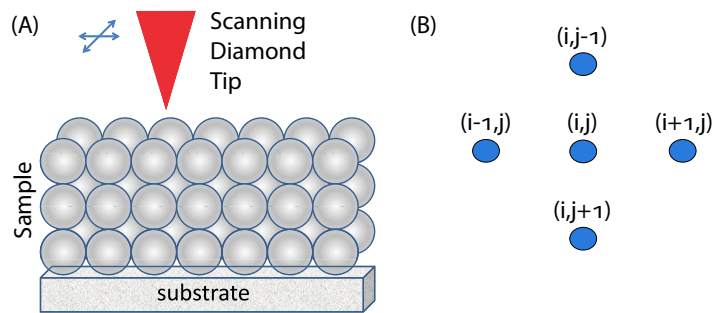
Figure 1. (A) Experimental setup for surface diamond magnetometry of clusters. The diamond is scanned across the surface, and surface magnetism is measured by subtracting the background signal from neighboring points (B). (Or, equivalently, the sample can be translated rather than the tip.)

the surface and performing background subtractions using neighboring points (figure 1(B)). An equivalent scheme is to translate the sample rather the tip. Nanodiamonds with a single NV center could be used, but so could nanocrystals containing multiple NV centers. For detecting superconducting phase transitions, we envisage an experiment in which both the external field and the sample temperature are cycled.

As the cluster size increases the properties approach those of the bulk. A bulk material consisting of embedded superconducting clusters may exhibit properties that are closer to those of a bulk superconducting material in the sense that diamagnetic effects can be enhanced compared to those of the individual clusters. Strong fields may not be needed in order to generate an observable magnetic moment if diamagnetism is created by persistent currents. In this case, the Meissner effect can be detected using a small external field.

We now look at ways of measuring the Meissner diamagnetism in a weak field using a diamond magnetometer. The experimental setup is shown in figure 2. Green light (532 nm) from a 200 mW continuous-wave solid-state laser is incident normal to the surface of a [111]-oriented diamond crystal of dimensions $2 \times 2 \times 1$ mm. The diamond was fabricated commercially by Sumitomo by the high-pressure, high-temperature (HPHT) method with an initial concentration of nitrogen impurities of less than 100 ppm, irradiated with a dose of 10^{19} cm^{-2}, 3.0 MeV electrons, then annealed for 2 h at 700 °C [36] to create NV centers. The fluorescence emitted by the diamond is recorded using a Si photodiode. A 675 ± 75 nm interference filter is used to attenuate the green light backscattered towards the photodiode. The BSCCO sample (BSCCO-2223, $Bi_2Sr_2Ca_2Cu_3O_{10}$), a 2.8 cm diameter, 4 mm thick disc, is placed at a distance of approximately 5 mm behind the diamond and parallel to the 2×2 mm face of the diamond. This particular sample-diamond geometric arrangement results in the largest magnetic-field shift due to the Meissner effect. An ambient bias field was generated by a coil that surrounded the experimental setup and produced ~ 14 G at the diamond's location.

The diamond was glued to a thin glass slide that was mounted on a printed circuit board with microwave striplines. A 200 microns diameter copper wire ran in between striplines ~ 1 mm from the surface of the diamond and delivered a cw microwave field (~ 13 dBm power, 2.895–2.915 GHz frequency-sweep range and 0.20 s sweep repetition time) from a Hewlett Packard 8350B sweep oscillator with an HP 83525B RF Plug-In module. The photocurrent from
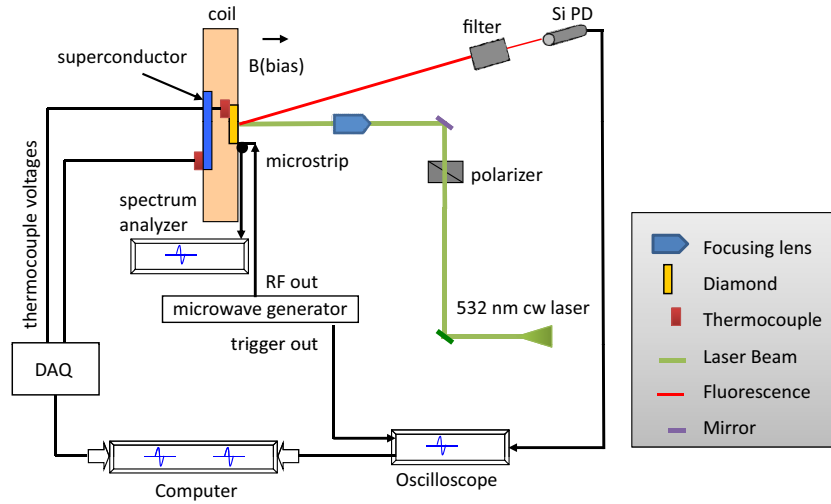
Figure 2. Schematic diagram of the experimental setup.

the Si photodiode was recorded using an oscilloscope triggered upon each microwave frequency sweep. A Labview interface was used to download the data from the oscilloscope and record thermocouple voltages at regular intervals. Two Type-T thermocouples were used to measure the temperature. The first thermocouple was placed within 1 mm of the diamond. The second was held in close contact with the BSCCO sample, and a silicon-based heatsink compound was used to improve thermal contact between the thermocouple and the superconductor.

Plots of the photocurrent versus microwave frequency are shown in figure 3 for various BSCCO sample temperatures. For each such graph, the $|m_S = 0\rangle \leftrightarrow |m_S = 1\rangle$ transition frequency from the [111]-oriented NV centers was extracted by fitting a set of three Lorentzian lines separated by 2.2 MHz corresponding to the hyperfine splitting due to the ^{14}N nuclei (spin $I = 1$), which can be found in three possible orientations $|m_I = 0\rangle$, $|m_I = \pm 1\rangle$ with respect to the NV axis [36]–[38].

The $|m_S = 0\rangle \leftrightarrow |m_S = 1\rangle$ transition center frequency provides a measure of the projection of the local magnetic field $\vec{B}$ along the NV axis, which causes a frequency shift $g\mu_B \vec{S} \cdot \vec{B}$, where $S = 1$ (spin) and the magnetogyric ratio $g\mu_B$ is $\approx 2.8\,\text{MHz G}^{-1}$ for the NV center electronic triplet spin state. This Zeeman splitting is in addition to the ZFS, $H_{cf} = D[S_z^2 - (1/3)S(S + 1)]$, with $D \approx 2.87\,\text{GHz}$ along the axis of the NV center (spin $S = 1$). For a superconductor below T_c placed in a bias field, we expect the Meissner effect to alter the magnetic field around it, due to the exclusion effect of the superconductor.

Our experiment consists of cooling the BSCCO sample in liquid nitrogen for 30 s and then rapidly positioning it in close proximity (5 mm) to the diamond crystal, with the disc parallel to the crystal plane. The disc's axis is parallel to $\vec{B}$. As the BSCCO sample warms up to room temperature, measurements of the $|m_S = 0\rangle \leftrightarrow |m_S = 1\rangle$ transition in diamond are carried out at regular intervals (every 4 s). With BSCCO-2223, T_c is 105 K [39], and this gives us nearly 20 s at ambient temperature to acquire measurements in the presence of the Meissner effect before the phase transition is crossed ($T > T_c$) and the superconductive state is lost. The results of four different runs performed under similar conditions are shown in figure 4. This protocol worked well for BSCCO, but for other materials, a better control of temperature, e.g. using a cryostat, may be required.
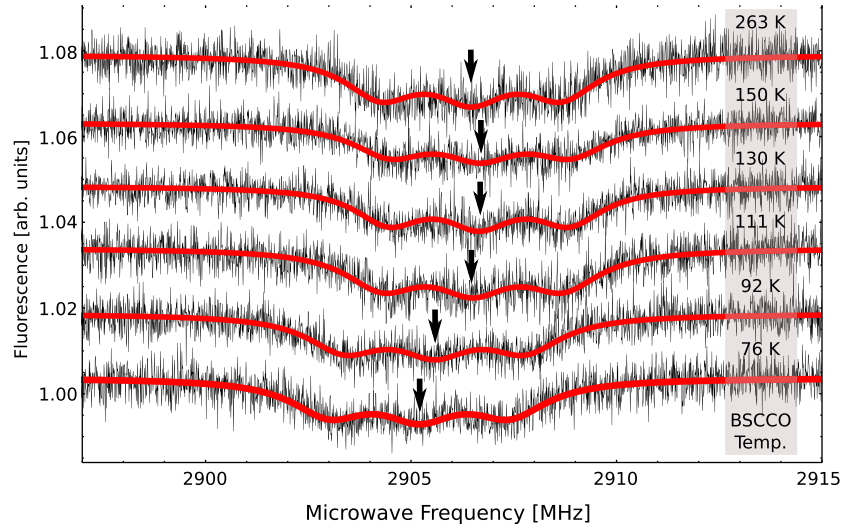
Figure 3. NV-diamond detected microwave spectroscopy of the $|m_S = 0\rangle \leftrightarrow |m_S = 1\rangle$ transition for different BSCCO temperatures. Three peaks can be resolved which correspond to the hyperfine splitting from the ^{14}N nucleus. Depending on the temperature of the BSCCO superconductor, the center of the $|m_S = 0\rangle \leftrightarrow |m_S = 1\rangle$ transition changes due to two competing effects: the Zeeman shift associated with the Meissner effect and a frequency shift associated with the diamond temperature, which may change as a result of the proximity to the BSCCO. See text for details.
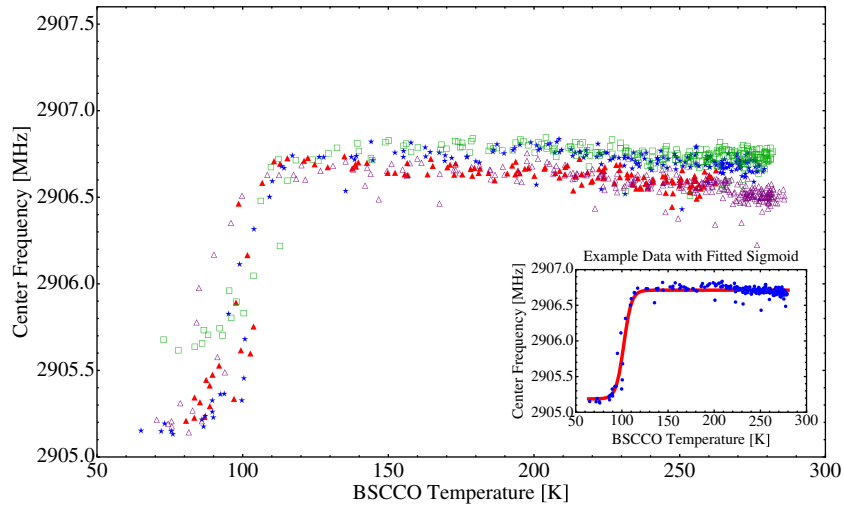

Figure 4. BSCCO-2223 shows a phase transition to the superconducting state at T_c of (102 ± 3) K. The four symbol types represent repeated runs on the same sample performed at different times.

The inset of figure 4 shows the least-squares fit of the data to a phenomenological sigmoid function

$$f(T) = \frac{f_1}{1 + \exp\left[-(T - T_c)/\tau\right]} + f_0 \tag{6}$$

Table 1. Results of the least-squares fit of a sigmoid to find the critical temperature. From these data, we find T_c of (102 ± 3) K.

Run	f_1 (MHz)	T_c (K)	τ (K)	f_0 (MHz)
1	1.3746	101.3	4.53	2905.3
2	1.5251	102.1	4.20	2905.2
3	1.0883	104.3	4.71	2905.7
4	1.4003	91.4	5.33	2905.2

for one particular run. The free parameters of the fit are T_c, f_0 and f_1. T_c indicates the phase transition; f_0 and f_1 are vertical offset and scaling parameters, respectively. The results for four runs are shown in table 1. From the fitted value of T_c, we determine a standard deviation of 5.7 K. The average value of T_c is 102 K.

Control experiments were performed with a Teflon disc cut to the same dimensions as the BSCCO sample and cooled to liquid nitrogen temperature. Results (not shown) did not exhibit any signs of a phase transition up to room temperature, as one would expect of a nonsuperconducting material.

The data in figure 4 show a typical spread in the $|m_S = 0\rangle \leftrightarrow |m_S = 1\rangle$ transition frequency measurements found in our experiments. This spread is seen to be of the order of about 50–100 kHz in the high temperature range. Part of this drift is caused by drifts of the diamond temperature towards colder temperatures, which we estimate to be at most about 10 K, as the cold sample is in close proximity to the diamond.

While performing the experiments in this study, we noticed a statistically significant dependence of the ZFS parameter D of the NV center on temperature. This indicates that extra care should be taken in variable temperature studies, for the effects of dD/dT are otherwise indistinguishable from changes in the external field in the scheme we have used here. The problem could be mitigated or eliminated either by subtraction of the effects of a temperature drift from independent measurements of temperature or by using gradiometer schemes. We have subsequently investigated the temperature dependence in detail and discussed possible ways of mitigating the effects [40].

In conclusion, we have demonstrated the use of NV-diamond magnetometry for probing the Meissner effects in a bulk superconductor and identified some issues associated with such experiments. When positioned in close proximity to the surface of a superconductor, changes in the surface field can be detected with temperature. Care must be taken to ensure that the temperature dependence of the ZFS parameters does not adversely affect the measurement.

We also estimate that it should be possible to probe magnetism in individual metal clusters. Nanoscale diamonds with NV color centers present a unique opportunity for the study of magnetism and superconductivity in nanomaterials, where sufficient resolution and sensitivity to observe the properties of individual clusters could be obtained. Other scanning probe techniques such as spin-polarized scanning tunneling microscopy (STM) [41] or magnetic resonance force microscopy (MRFM) [42] could also potentially be used, with their own advantages and disadvantages. (For example, STM requires a conductive sample, whereas superconductors are poor conductors in their normal state.) A detailed comparison with other potential techniques is beyond the scope of this paper.

In bulk superconductors, nanoscale NV-diamond magnetometry could be used to image vortices, paramagnetism and nucleation effects and could present advantages over micro-SQUID scanning techniques [43] by enabling variable temperature and hysteresis studies while maintaining close proximity to the sample throughout the cycle. NMR parameters T_1, T_2 and chemical shift could also be measured to probe the nature of the order parameter, which is known to exhibit heterogeneities at a local level. Most importantly, high temperatures are inaccessible to SQUIDs without the use of thermal insulation layers that would prevent short-distance operation. While nucleation effects in the paramagnetic Meissner effect are known to depend on the cooling rate [43] and most likely exhibit hysteresis effects, magnetic imaging studies have not been carried out as a function of temperature across the phase transition. Such studies could shed light on the origins of the paramagnetism. Finally, the study of individual metal clusters and their interaction with the environment and surfaces could help us to understand their roles in chemical catalysis.

Acknowledgments

References

[1] Ginzburg V 2005 *Phys.-Usp.* **48** 173
[2] Chu C, Chen F, Shulman J, Tsui S, Xue Y, Wen W and Sheng P 2005 arXiv:cond-mat/0511166v1
[3] Pickett W 2006 *J. Supercond.* **19** 291
[4] Zakhidov A *et al* 1998 *Science* **282** 897
[5] Reyren N *et al* 2007 *Science* **317** 1196
[6] de Heer W 1993 *Rev. Mod. Phys.* **65** 611
[7] Kresin V and Knight W 1998 *Z. Phys. Chem.* **203** 67
[8] Brack M 1993 *Rev. Mod. Phys.* **65** 677
[9] Ovchinnikov Y and Kresin V 2005 *Eur. Phys. J.* B **45** 5
[10] Kresin V and Ovchinnikov Y 2008 *Phys.-Usp.* **51** 427
[11] Cao B, Neal C, Starace A, Ovchinnikov Y, Kresin V and Jarrold M 2008 *J. Supercond. Nov. Magn.* **21** 163
[12] Sergeeva-Chollet N, Dyvorne H, Polovy H, Pannetier-Lecoeur M and Fermon C 2010 *IFMBE Proc., 17th Int. Conf. on Biomagnetism Advances in Biomagnetism Biomag 2010* vol 28 ed S Supek and A Susac (Berlin: Springer) pp 70–3
[13] Dyvorne H, Fermon C, Pannetier-Lecoeur M, Polovy H and Walliang A 2009 *IEEE Trans. Appl. Supercond.* **19** 819
[14] Balasubramanian G *et al* 2008 *Nature* **455** 648
[15] Balasubramanian G *et al* 2009 *Nat. Mater.* **8** 383
[16] Maze J *et al* 2008 *Nature* **455** 644
[17] Cao B, Neal C M, Starace A K, Ovchinnikov Y N, Kresin V Z and Jarrold M F 2008 arXiv:0804.0824
[18] Breaux G *et al* 2005 *Phys. Rev. Lett.* **94** 173401
[19] Weitz I, Sample J, Ries R, Spain E and Heath J 2000 *J. Phys. Chem.* B **104** 4288
[20] Hebel L and Slichter C 1959 *Phys. Rev.* **113** 1504
[21] Vega A J, Beckmann P A, Bai S and Dybowski C 2006 *Phys. Rev.* B **74** 214420

IOP Institute of Physics Φ DEUTSCHE PHYSIKALISCHE GESELLSCHAFT

[22] Hagel J 2002 *J. Low Temp. Phys.* **129** 133

[23] Duffe S, Irawan T, Bieletzki M, Richter T, Sieben B, Yin C, von Issendorff B, Moseler M and Hövel H 2007 *Eur. Phys. J.* D **45** 401

[24] Partridge J, Reichel R, Ayesh A, Mackenzie D and Brown S 2006 *Phys. Status Solidi* a **203** 1217

[25] Yin S, Moro R, Xu X and de Heer W 2007 *Phys. Rev. Lett.* **98** 113401

[26] Kittel C 2004 *Introduction to Solid State Physics* 8th edn (New York: Wiley)

[27] Neumann P, Beck J, Steiner M, Rempp F, Fedder H, Hemmer P, Wrachtrup J and Jelezko F 2010 *Science* **329** 542

[28] Stanwix P L, Pham L M, Maze J R, Le Sage D, Yeung T K, Cappellaro P, Hemmer P R, Yacoby A, Lukin M D and Walsworth R L 2010 *Phys. Rev. B* **82** 201201(R)

[29] Epstein R J, Mendoza F M, Kato Y K and Awschalom D D 2005 *Nat. Phys.* **1** 94–8

[30] Huber M, Koshnick N, Bluhm H, Archuleta L, Azua T, Bjornsson P, Gardner B, Halloran S, Lucero E and Moler K 2008 *Rev. Sci. Instrum.* **79** 053704

[31] Eesley G, Heremans J, Meyer M and Doll G 1990 *Phys. Rev. Lett.* **65** 3445

[32] Hartley P, Thissen H, Vaithianathan T and Griesser H 2000 *Plasmas Polym.* **5** 47

[33] Dulkeith E, Ringler M, Klar T and Feldmann J 2005 *Nano Lett.* **5** 585

[34] Siyushev P *et al* 2010 arXiv:1009.0607v1 [quant-ph]

[35] Hadden J, Harrison J, Stanley-Clarke A, Marseglia L, Ho Y, Patton B, O'Brien J and Rarity J 2010 arXiv:1006.2093 [quant-ph]

[36] Acosta V *et al* 2009 *Phys. Rev.* B **80** 115202

[37] Wei C and Manson N 1999 *J. Opt. B: Quantum Semiclass. Opt.* **1** 464

[38] Manson N, Harrison J and Sellars M 2006 *Phys. Rev. B* **74** 104303

[39] Lim H and Byrne J 1997 *Metall. Mater. Trans.* B **28** 425

[40] Acosta V, Bauch E, Ledbetter M, Waxman A, Bouchard L and Budker D 2010 *Phys. Rev. Lett.* **104** 070801

[41] Bode M 2003 *Rep. Prog. Phys.* **66** 523

[42] Degen C L, Poggio M, Mamin H J, Rettner C T and Rugar D 2009 *Proc. Natl Acad. Sci. USA* **106** 1313

[43] Kirtley J, Mota A, Sigrist M and Rice T 1998 *J. Phys.: Condens. Matter* **10** L97

[44] Steiner M, Neumann P, Beck J, Jelezko F and Wrachtrup J 2010 *Phys. Rev.* B **81** 035205

[45] Jiang L, Hodges J, Maurer J M P, Taylor J, Cory D, Hemmer P, Walsworth R, Yacoby A, Zibrov A and Lukin M 2009 *Science* **326** 267